Two-dimensional effects in Fowler-Nordheim field emission from transition metal dichalcogenides

IOP Conf. Series: Journal of Physics: Conf. Series **1226** (2019) 012018 doi:10.1088/1742-6596/1226/1/012018

Two-dimensional effects in Fowler-Nordheim field emission from transition metal dichalcogenides

F Urban[1,3], M Passacantando[2,3], F Giubileo[3], L Iemmo[1,3], G Luongo[1,3], A Grillo[1], A Di Bartolomeo[1,3]*

[1] Department of Physics "E.R. Caianiello", University of Salerno, 84084, Fisciano, Italy;
[2] Department of Physical and Chemical Science, University of L'Aquila, and CNR-SPIN L'Aquila, via Vetoio, Coppito 67100, L'Aquila, Italy;
[3] CNR-SPIN Salerno, 84084, Fisciano, Italy;
* Correspondence: adibartolomeo@unisa.it; Tel.: +39-089-969-189

Abstract. We report field emission from bilayer MoS_2 and monolayer WSe_2 synthesized by CVD on SiO_2/Si substrate. We show that the emitted current follows a Fowler-Nordheim model modified to account for the two-dimensional confinement of charge carriers. We derive the figures of merit of field emission and demonstrate that few-layer transition-metal dichalcogenides are suitable for field emission applications.

1. Introduction

Transition - metal dichalcogenides (TMDs), chemical formula $\boldsymbol{MX_2}$, have been largely investigated during the last few years. They present a layered structure, characterized by a honeycomb lattice where each transition metal $\boldsymbol{M}$ ($\boldsymbol{Mo, W, We}$, **etc**.) is covalently bonded to two chalcogenide atoms $\boldsymbol{X}$ ($\boldsymbol{S, Se, Te}$). TMDs have been intensively studied for the ease of fabrication and the tuneable and sizeable bandgap suitable for optoelectronic applications [1,2]. Like graphene, TMDs can be mechanically exfoliated from a bulk material and transferred on a substrate [3]; however, single-crystal and large-scale flakes, with controlled number of layers, are more easily produced by chemical vapor deposition (CVD) [4]. Those materials are considered good candidates for technological applications because they offer good control on of the energy bandgap through the number of layers [5], which increases passing from bulk to monolayer form, high on/off ratio ($> 10^7$) [6] and low subthreshold swing (below $70\ \mathrm{mV/decade}$) [7,8], even though their mobility is typically only few tens $\mathrm{cm^2V^{-1}s^{-1}}$[9,10]. Their strong light absorption and emission open the route for high-responsivity photodetectors, high-intensity light emitters and efficient photovoltaic cells [11,12]. Furthermore, the intrinsic sharp edges due to the 2D nature and the low work function enable field emission applications. Anyway, unlike graphene and carbon nanotubes (CNTs) [13,14], TMDs have not been much explored as cold cathodes for applications in vacuum electronics, flat panel displays, electron microscopy, x-ray tubes [15–17], etc. Only few studies focussed on field emission

from MoS_2 and WSe_2 have been reported to date [18–20]. In this paper, we investigate the field emission (FE) behaviour of MoS_2 and WSe_2 bilayer and monolayer flakes. Specifically, we report FE measurements from their flat part. We show that the experimental data are well fitted by a Fowler-Nordheim (FN) model [21] modified to take into account the two-dimensional (2D) nature of the material. We derive the characteristic FE parameters such as the field enhancement factor β and the turn on field to show that TMDs are promising materials for field emission applications.

2. Materials and Methods

We grew the two analysed samples, $\boldsymbol{MoS_2}$ and $\boldsymbol{WSe_2}$ flakes, by chemical vapor deposition on a highly p-doped $\boldsymbol{Si}$ substrates covered by $\boldsymbol{300\ nm}$ of $\boldsymbol{SiO_2}$ (silicon dioxide). The CVD growths, at 850 °C, were performed in a two-zone quartz tube furnace, with the substrate placed face down on the transition-metal precursor and the chalcogen carried by an Ar gas flow [22]. Flakes were randomly formed on the substrates. Figure 1(a) and Figure 1(b) show SEM images of two selected flakes, $\boldsymbol{MoS_2}$ and $\boldsymbol{WSe_2}$, respectively. The field emission measurements were performed in the SEM chamber, at a pressure $\boldsymbol{< 10^{-6}\ mbar}$, exploiting the piezo-controlled tungsten tip ($\boldsymbol{W}$-tip) movement for the accurate positioning of the anode in front of the emitting flake (cathode) at a close distance $\boldsymbol{d}$, as displayed in insets of Figure 1(a) and (b).

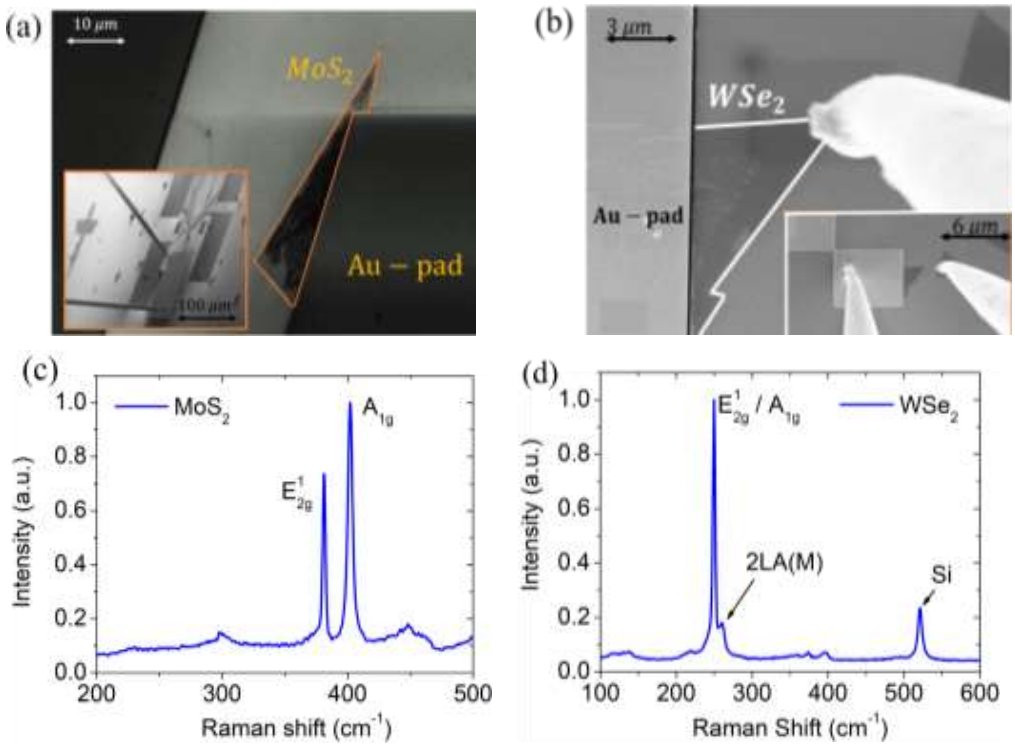

Figure 1. SEM images of the flakes used for field emission measurements and in insets the position of the tungsten tips: the lower one on the metal pad contacting the flake, the other placed in front of the flake at a close distance *d*, respectively for MoS_2(a) and WSe_2(b). Raman spectra of the MoS_2(c) and WSe_2(d).

The flakes were characterized by Raman spectroscopy with an unpolarized incident laser to identify the number of layers. The Raman spectrum reported in Figure 1(c), referring to MoS_2, shows two peaks at $\sim 381\ cm^{-1}$ and $\sim 401\ cm^{-1}$ which are associated with the in-plane vibrations of sulfur atoms (E^1_{2g}) and with the out-of-plane vibrations of Mo and S atoms (A_{1g}), respectively [23]. The separation of $\sim 20\ cm^{-1}$ indicates bilayer flakes. Similarly, Figure 1(d) shows the Raman spectrum of the WSe_2 flake. It exhibits two peaks around $\sim 250\ cm^{-1}$ and $\sim 260\ cm^{-1}$, corresponding the

first to a combination of the in-plane vibrations of W and Se atoms (E_{2g}) and out-of-plane vibrations of Se atoms (A_{1g}), and the other one to a second order resonant Raman mode ($2\,LA\,(M)$) due to LA phonons at the M point in the Brillouin zone [24]. The peak frequency positions are compatible with WSe_2 monolayer, which was further confirmed by photoluminescence measurements (not shown here) [18].

3. Results

Considering that the MoS_2 and WSe_2 flakes are naturally n-doped and that the sharp edges or nano-protrusions of the flat-part can originate a high electric field amplification [14,25], we expect easy extraction of electrons upon application of a voltage.

According to the standard FN theory [26] the field emission current usually results in a linear $\ln(I_{ds}/(V_{ds}^2))$ vs. $1/V_{ds}$ FN plot. However, for 2D materials, it has been proposed [21] that a modified FN model has to be applied to the vertical electron emission to take into account the reduced dimensionality, the energy spectrum, the non-conserving in-plane electron momentum, the finite-temperature and the space-charge-limited effects.

The modified FN model results in the following field emission current

$$I_{FN}^{2D} = A_{FN}^{2D} \exp\left[-\frac{b\Phi^{\frac{3}{2}}}{\beta E}\right] \quad (1)$$

where A_{FN}^{2D} and b are constants, S and ϕ represent the emitting surface and the electron affinity (in our case $\phi = 4.2\,eV$ for MoS_2 [27] and $3.9\,eV$ for WSe_2 [28]), β is the so-called field enhancement factor, a typical figure of merit for the qualification of field emitter material. Finally, the electric field is $E = V/d$, where V represents the anode-cathode voltage and d their distance.

For both samples the FE current was measured with the (anode) W-tip positioned at a fixed distance ($d{\sim}200\,nm$ for MoS_2 and $d \sim 400\,nm$ for WSe_2) from the surface (inner flat part of the flake). We disregarded the edges after having verified that the oxidation after air exposure and the higher concentration of unreacted precursor (MO_x and WO_x) had hampered the extraction of electrons from them. The current was monitored during the voltage sweep up to 120 V (a constraint to avoid the oxide breakdown).

Figure 2(a) and 2(b) show that, when V is below a critical value, the current fluctuates around the noise floor $< 10^{-13}A$, and there is no measurable signal. For $V_{ds} > V_{th}$ an exponential increase (well visible in insets of Figure 2(a) and (b)) in the current is observed. The current-voltage characteristics show the typical fluctuations of emission current, related to desorption of adsorbates caused by Joule heating.

The fits of the experimental data at high-field regime of eq.1 are shown in Figure 2(c) and 2(d) compared with the 3D Fowler-Nordheim model [26], reported in inset. The accuracy of the linear fit is evaluated with the $\chi^2 \sim 0.99$, defining a good agreement in a wide range of voltage values, slightly better for WSe_2 respect to the classical 3D Fowler-Nordheim model.

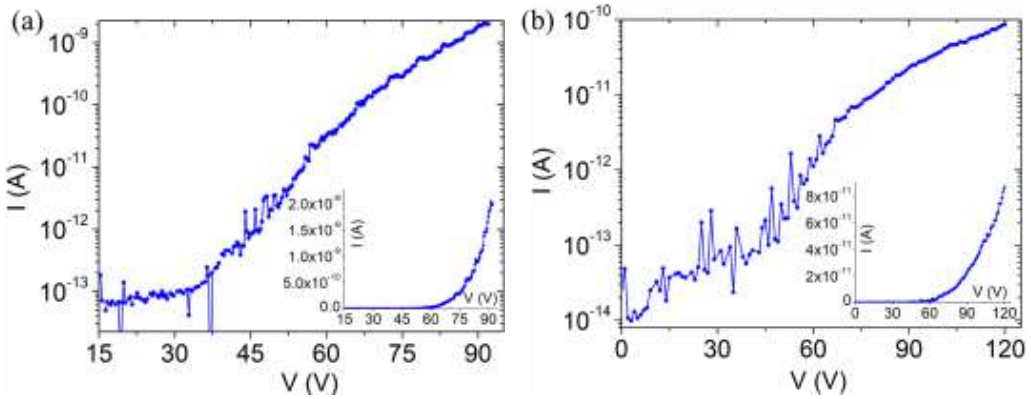

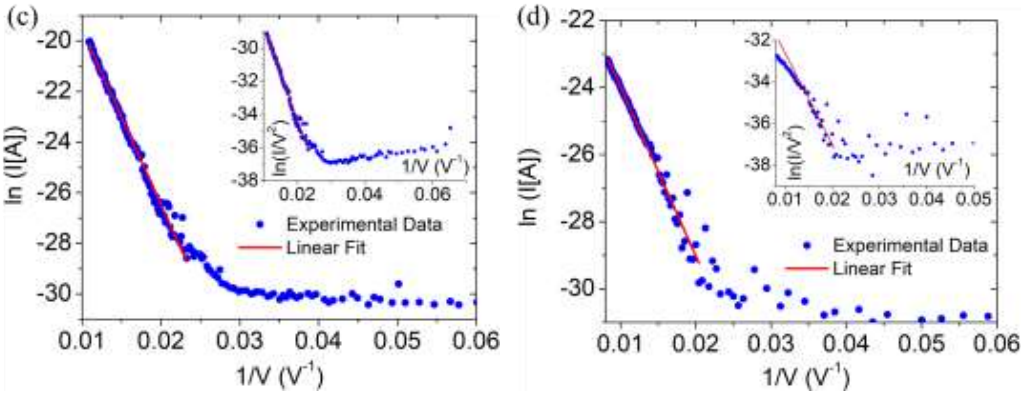

Figure 2. Field emission curves plotted in logarithmic scale as a function of anode-cathode voltage and linear scale (inset) for MoS_2(a) and WSe_2(b). Experimental data (blue circles) and model fit (red lines) of field emission measures for MoS_2(c) and WSe_2(d). The insets show the comparison of the experimental data fitted with standard Fowler-Nordheim model.

Indeed, this provides an indication in favour of the 2D modified FN model proposed in ref. [21], that should be further addressed and confirmed in future experiments.
From the slopes of the linear fits (eq.1) we derive the field enhancement factor $\beta = -b\, d\, \phi^{3/2}/m \sim 17$ and ~ 40 for MoS_2 and WSe_2 respectively.
The seemingly low values of the amplification factor (good emitters reach $\beta \sim 1000$ or more) are remarkable if we consider that emission happens from the inner part of the flake, without taking advantage from the 2D shape of the flake. Despite that, the turn-on field, defined as the field applied to extract a current of 1 pA has a value of $\sim 230\, V/\mu m$ and $150\, V/\mu m$ for MoS_2 and WSe_2, respectively, which are rather low compared to the typical turn on field of several $kV/\mu m$ needed to extract electrons from flat surfaces. These results demonstrate the MoS_2 and WSe_2 suitability as field emitters.

4. Conclusion

In conclusion, we have fabricated MoS_2 bilayers and WSe_2 monolayer flakes and analysed their field emission properties. We have demonstrated that a modified field emission model, which considers the 2D nature of the flakes, provides a slightly better agreement with the experimental data compared to the original Fowler-Nordheim model, opening the route for further investigations. We have highlighted that TMDs are promising materials not only for electronics and optoelectronics but also for field emission applications.

References

[1] Di Bartolomeo A, Genovese L, Giubileo F, Iemmo L, Luongo G, Tobias Foller and Schleberger M 2018 Hysteresis in the transfer characteristics of MoS 2 transistors *2D Materials* **5** 015014

[2] Pospischil A and Mueller T 2016 Optoelectronic Devices Based on Atomically Thin Transition Metal Dichalcogenides *Applied Sciences* **6**

[3] Lin Z, McCreary A, Briggs N, Subramanian S, Zhang K, Sun Y, Li X, Borys N J, Yuan H, Fullerton-Shirey S K, Chernikov A, Zhao H, McDonnell S, Lindenberg A M, Xiao K, LeRoy B J, Drndić M, Hwang J C M, Park J, Manish Chhowalla, Schaak R E, Javey A, Hersam M C, Robinson J and Terrones M 2016 2D materials advances: from large scale synthesis and controlled heterostructures to improved characterization techniques, defects and applications *2D Materials* **3** 042001

[4] Feng Y, Zhang K, Wang F, Liu Z, Fang M, Cao R, Miao Y, Yang Z, Mi W, Han Y, Song Z and Wong H S P 2015 Synthesis of Large-Area Highly Crystalline Monolayer Molybdenum

Disulfide with Tunable Grain Size in a H2 Atmosphere *ACS Applied Materials & Interfaces* **7** 22587–93

[5] Mak K F, Lee C, Hone J, Shan J and Heinz T F 2010 Atomically Thin MoS2: A New Direct-Gap Semiconductor *Phys. Rev. Lett.* **105** 136805

[6] Zhou C, Wang X, Raju S, Lin Z, Villaroman D, Huang B, Chan H L-W, Chan M and Chai Y 2015 Low voltage and high ON/OFF ratio field-effect transistors based on CVD MoS2 and ultra high-k gate dielectric PZT *Nanoscale* **7** 8695–700

[7] Nourbakhsh A, Zubair A, Joglekar S, Dresselhaus M and Palacios T 2017 Subthreshold swing improvement in MoS2 transistors by the negative-capacitance effect in a ferroelectric Al-doped-HfO2/HfO2 gate dielectric stack *Nanoscale* **9** 6122–7

[8] Fang H, Chuang S, Chang T C, Takei K, Takahashi T and Javey A 2012 High-Performance Single Layered WSe2 p-FETs with Chemically Doped Contacts *Nano Lett.* **12** 3788–92

[9] Lopez-Sanchez O, Lembke D, Kayci M, Radenovic A and Kis A 2013 Ultrasensitive photodetectors based on monolayer MoS2 *Nature Nanotechnology* **8** 497

[10] Zhou H, Wang C, Shaw J C, Cheng R, Chen Y, Huang X, Liu Y, Weiss N O, Lin Z, Huang Y and Duan X 2015 Large Area Growth and Electrical Properties of p-Type WSe2 Atomic Layers *Nano Lett.* **15** 709–13

[11] Zheng Z, Zhang T, Yao J, Zhang Y, Xu J and Yang G 2016 Flexible, transparent and ultra-broadband photodetector based on large-area WSe 2 film for wearable devices *Nanotechnology* **27** 225501

[12] Di Bartolomeo A, Genovese L, Foller T, Giubileo F, Luongo G, Luca Croin, Liang S-J, Ang L K and Schleberger M 2017 Electrical transport and persistent photoconductivity in monolayer MoS 2 phototransistors *Nanotechnology* **28** 214002

[13] Di Bartolomeo A, Giubileo F, Iemmo L, Romeo F, Russo S, Unal S, Passacantando M, Grossi V and Cucolo A M 2016 Leakage and field emission in side-gate graphene field effect transistors *Appl. Phys. Lett.* **109** 023510

[14] Iemmo L, Di Bartolomeo A, Giubileo F, Luongo G, Passacantando M, Niu G, Hatami F, Skibitzki O and Schroeder T 2017 Graphene enhanced field emission from InP nanocrystals *Nanotechnology* **28** 495705

[15] Giubileo F, Di Bartolomeo A, Iemmo L, Luongo G, Passacantando M, Koivusalo E, Hakkarainen T V and Guina M 2017 Field Emission from Self-Catalyzed GaAs Nanowires *Nanomaterials* **7**

[16] Yabushita R, Hata K, Sato H and Saito Y 2007 Development of compact field emission scanning electron microscope equipped with multiwalled carbon nanotube bundle cathode *Journal of Vacuum Science & Technology B: Microelectronics and Nanometer Structures Processing, Measurement, and Phenomena* **25** 640–2

[17] Gupta A P, Park S, Yeo S J, Jung J, Cho C, Paik S H, Park H, Cho Y C, Kim S H, Shin J H, Ahn J S and Ryu J 2017 Direct Synthesis of Carbon Nanotube Field Emitters on Metal Substrate for Open-Type X-ray Source in Medical Imaging *Materials* **10** 878

[18] Di Bartolomeo A, Urban F, Passacantando M, McEvoy N, Peters L, Iemmo L, Luongo G, Romeo F and Giubileo F 2018 A WSe2 vertical field emission transistor *ArXiv e-prints*

[19] Urban F, Passacantando M, Giubileo F, Iemmo L and Di Bartolomeo A 2018 Transport and Field Emission Properties of MoS2 Bilayers *Nanomaterials* **8**

[20] Gaur A P S, Sahoo S, Mendoza F, Rivera A M, Kumar M, Dash S P, Morell G and Katiyar R S 2016 Cold cathode emission studies on topographically modified few layer and single layer MoS2 films *Applied Physics Letters* **108** 043103

[21] Sin Ang Y, Zubair M, Ooi K J A and Ang L K 2017 Generalized Fowler-Nordheim field-induced vertical electron emission model for two-dimensional materials *arXiv:1711.05898*

[22] O'Brien M, McEvoy N, Hallam T, Kim H-Y, Berner N C, Hanlon D, Lee K, Coleman J N and Duesberg G S 2014 Transition Metal Dichalcogenide Growth via Close Proximity Precursor Supply *Scientific Reports* **4** 7374

[23] Li X and Zhu H 2015 Two-dimensional MoS2: Properties, preparation, and applications *Journal of Materiomics* **1** 33–44

[24] O'Brien M, McEvoy N, Hanlon D, Hallam T, Coleman J N and Duesberg G S 2016 Mapping of Low-Frequency Raman Modes in CVD-Grown Transition Metal Dichalcogenides: Layer Number, Stacking Orientation and Resonant Effects *Scientific Reports* **6** 19476

[25] Di Bartolomeo A, Passacantando M, Niu G, Schlykow V, Lupina G, Giubileo F and Schroeder T 2016 Observation of field emission from GeSn nanoparticles epitaxially grown on silicon nanopillar arrays *Nanotechnology* **27** 485707

[26] Fowler R H and Nordheim L 1928 Electron emission in intense electric fields *Proc R Soc London A* **119** 173–81

[27] Choi S, Shaolin Z and Yang W 2014 Layer-number-dependent work function of MoS2 nanoflakes *Journal of the Korean Physical Society* **64** 1550–1555

[28] Smyth C M, Addou R, McDonnell S, Hinkle C L and Wallace R M 2017 WSe 2 -contact metal interface chemistry and band alignment under high vacuum and ultra high vacuum deposition conditions *2D Materials* **4** 025084